Translocation of a stiff polymer in a microchannel

A. ten Bosch* and P. Cheyssac
Laboratoire de Physique de la Matiere Condensee, CNRS 6622, Parc Valrose, F-06108 Nice Cedex 2, France
(Received 6 July 2008; published 8 January 2009)

The voltage-driven dynamics of a stiff polymer through a nanopore are treated with a bend elastic model. In contrast to flexible polymers described by a stretch elasticity, bend elastic chains can be oriented in an external field, here the anchoring field created by the pore atoms. The trajectory of the chain is calculated using the Langevin equation of motion. The dynamical equation is solved by a normal mode analysis of the elastic curve with free ends. Interaction with the pore walls acts to align the chain, and with the electric field induced inside the pore controls the translocation time. Application of a force proportional to the distance of the exit from the end of the pore such as an optical trap slows down the motion, and reduces the chain response to the wall potential and the extension along the pore axis. DNA is a well-known semirigid polymer, and a comparison is made to the molecular dynamics simulation of translocation of DNA through a synthetic nanopore.

DOI: 10.1103/PhysRevE.79.011903 PACS number(s): 87.15.hj, 87.16.ad, 87.16.dp

I. INTRODUCTION

Industrial applications based on the flow of dilute solutions of polymers in pores of diameters ranging from nanometers to micrometers are ubiquitous. Recent work has concentrated on the dynamics and structure of biopolymers, in particular as a tool for the analysis and manipulation of DNA sequences [1,2]. Dynamics modeling should lead to predictive models of how macromolecules behave in microfluidic flows, useful for device design and optimization. In order to advance the technology it is essential to characterize the conformations of the macromolecule and the events taking place inside the pore in detail. Langevin dynamics is most commonly used and is based on rapid collisions of solvent and pore wall molecules with the diffusing Brownian particle [3–9]. The resulting loss of information with respect to a detailed molecular dynamics simulation [10–12] is offset by a relative ease of calculation. In order to fully describe dynamic phenomena either by analytical calculation or by numerical simulation, multiscale methods have also been proposed, and especially interesting is a first-principle calculation of the chemical structure of the single macromolecule to determine the parameters of the simple model used in an analytical method for the dynamics.

The dynamics of a polymer chain span a large range of time and length scales, from picoseconds and angstroms for the individual molecule segments to hours and centimeters for domain motion in polymer crystals. For example, in the spectrum of vibrations of a polymer on the scale of interatomic vibrations the series of discrete high-frequency lines is characteristic of the motion of the molecular building blocks of the chain. On the macroscopic level of acoustic waves, the details of the individual chain structure are not essential to the collective low-frequency modes. A continuum monomer density distribution with reasonable elastic coefficients will suffice to describe the wide spectrum of sound propagation in an elastic material. Of special interest is the range between these two limits. The relaxation of chain deformation superimposed on the drift caused by external sources determines the dynamics in dilute solution. Calculations assume a simple model chain structure with reasonable values of single chain friction, segment length, or elastic spring constants. Models that have been used with success are the elastic chain, the bead spring, or the bead rod polymer [13]. Unfortunately, only the dynamics of flexible chains are easy to manipulate and only if the motion of a single chain is decoupled from the surrounding chains. Most macromolecules are semirigid and resist bending, many have a helix structure, and this is especially true of the natural and biological polymers such as DNA, many of which even form liquid crystal phases.

The elastic wormlike chain has been used successfully to describe equilibrium properties of semirigid polymers [14–16]. The complex chemical structure of the macromolecule is replaced by an elastic chain of degree of polymerization N (or total arclength L), of stretch elastic coefficient κ, and bend elastic coefficient ϵ. The polymer conformation is described by a continuous chain given by positions $\vec{r}(s)$ at arclength s from the first monomer, with bend deformation described by the change in tangent vector $d^2\vec{r}/ds^2$ along the chain and stretch described by the change in position vector $\vec{dr}(s)/ds$. Early work already considered the coupling of the tangent vector to the local orientation and the validity of the relation valid for a geometric curve $|d\vec{r}/ds|=1$ [17–19]. The problem is still being explored, as well as the need to include bend and torsion of polymer chains in dynamic properties [20,21].

In rigid and semirigid systems the long-range intermolecular interaction depends on the relative orientation of the particles. In particular, in the neighborhood of a surface, an anchoring force determines a preference for a fixed direction relative to the surface [13,22–25]. In nanopores, the range of wall effects can easily extend over the whole pore width. The nature of the force can be steric, chemical with formation of covalent or ionic bonds, or electrostatic with formation of a surface charge or dipolar with induced or permanent dipoles. External fields such as an imposed electric field can also orient the semirigid polymer by coupling to the induced dipoles along the chain backbone [26]. For a charged polyelec-

*tenbosch@unice.fr

trolyte such as DNA, the electric field mainly works to pull the polymer through the pore, accelerating the otherwise slow random diffusion.

II. THEORY AND RESULTS

A. The Langevin equation

The Langevin equation of motion of the polymer inside the pore is

$$m\frac{\partial^2\vec{r}(s,t)}{\partial t^2}+m\zeta\frac{\partial\vec{r}(s,t)}{\partial t}+\epsilon\frac{\partial^4\vec{r}(s,t)}{\partial s^4}-\kappa\frac{\partial^2\vec{r}(s,t)}{\partial s^2}-\vec{F}-\vec{A}(s,t)=0. \quad (1)$$

The monomer mass is m and the first term is the inertia. The second term is the internal friction force. The next terms are the stretch and bend elasticity for the continuous elastic chain. The external force is given by $\vec{F}=\vec{F}_W+\vec{F}_E$; here the pore wall interaction $\vec{F}_W$ and the electric field $\vec{F}_E$. The last term on the left is the random force, here white noise $\vec{A}(s,t)$.

In stiff polymer chains the interaction between the polymer segments and the pore wall atoms can be expanded in spherical harmonics $Y_{lm}(u)$ in the orientation $d\vec{r}/ds=\vec{u}(s,t)$ of the monomer at position $\vec{r}(s,t)$ [22,27]. The position-dependent mean field component of order ℓ contains a short-range repulsive interaction and a long-range attraction perpendicular to the pore walls, and the derivative along the pore axis yields an effective friction force. Isotropic interactions will not be considered in the case of a pore width sufficiently large ($\geqslant$2 nm) and pore length sufficiently small. For a pore width larger than the diameter of the monomers, the isotropic potential $\ell=0$ forms a weak attractive well close to the pore walls and contributes a weak corrugation force. Wide pores also avoid significant overlapping and interaction between monomers during translocation [28]. The main effect of the pore walls is then to orient the monomers parallel to the axis along z of the nanopore [10]. Due to symmetry of the pore entrance and exit and of the head and tail polymer chain, the first orientation-dependent term for $\ell=2$ is then a function of u_z^2. The force in the z direction is then

$$F_{W,z}=\frac{W}{2}\left[3\left(\frac{\partial z}{\partial s}\right)^2-1\right]. \quad (2)$$

For orientation parallel to z, the average force must be positive and $W\geqslant 0$. The model mean field interaction parameter W describes the dominant friction force for a given distribution of pore atoms. For anchoring to occur along the pore axis, roughness (variations along the z axis) of pore walls is essential [29]. The average anchoring force is proportional to the stretch elastic stress tensor and vanishes for random orientation of bend elastic chains and for flexible Rouse chains.

The membrane with a single pore is placed in the center of the translocation cell. A constant voltage is applied between the two electrodes of the cell. Surface charges $\pm\sigma$ are induced on the surface of the dielectric membrane material by the external field $E_0=-\sigma/\epsilon_0$, strongly distorting the field at the pore entrance at $z=0$ [30–32]. A model for the electric field, discussed in the Appendix, is

$$E(z)=-\frac{\sigma}{\epsilon_0\epsilon_m}\left(\frac{z}{2\sqrt{z^2+R^2}}+\frac{H-z}{2\sqrt{(H-z)^2+R^2}}+\frac{\epsilon_m}{\epsilon_s}\right). \quad (3)$$

A uniform charge distribution $e<0$ on the polymer chain couples to the screened applied electric field; the electrostatic interaction between monomers is also screened by the counterions in the solvent [33,34]. Inside the pore, a coupling term $p_z dE(z)/dz$ with the permanent dipoles of the polymer of dipole moment p_z must be included in the total electrostatic force along z. An expansion is used and $F_{E,z}=F_0+F_1 z$. Using a parabolic fit to $E(z)$ in Eq. (3), F_0 and F_1 are found as functions of the parameters of $E(z)$:

$$F_0=eE(0)-\frac{4p_z}{3H}[E(H/2)-E(0)] \quad (4)$$

and

$$F_1H=-\frac{4}{3}[E(H/2)-E(0)]\left(e-\frac{2p_z}{H}\right). \quad (5)$$

The contribution of the dipole coupling term to F_0 and F_1 is of the order of 5% or less for the model pore electric field of Eq. (3) and the effective charge and dipole moments of DNA [1]. The effect could be larger if the gradient of the pore electric field is amplified, for example by pore geometry. Experiments have been made in the presence of an optical trap placed at the end of the pore. A field is created proportional to the distance of the chain from the pore end and an additional term proportional to the strength of the trap is contained in $F_1\leqslant 0$. If the polymer segments have an anisotropic polarizability $\Delta\alpha$, the external electric field couples to the monomer orientation $u_z(s)$ through the interaction $\epsilon_0\Delta\alpha\vec{E}^2[3(u_z)^2-1]/6$ [35]. The strength of the resulting force is of the order of $0.01kT$ or less in reasonable applied fields and much weaker than the effect of the pore wall atoms.

The parameters of the model are the geometry of the cylindrical pore (radius R and length H), the total length L of the polymer, the monomer size a, the elastic coefficients for bend ϵ and stretch κ, the monomer dipole moment $\vec{p}$ and effective charge e of the polymer, the external electric field E_0, the dielectric constants ϵ_m,ϵ_s of the pore membrane and the solvent and friction constant ζ of the solvent, and finally the strength W of the pore wall anchoring force. The interaction parameters are effective parameters which can be fitted to a given experimental system and for a given polymer are dependent on the material of the pore walls, the solvent and concentration of free ions. For example for DNA ϵ/kTa can vary between 50 and 150 nm for decreasing salt concentration [4,36,37].

The model equation along the pore axis is then

$$m\frac{\partial^2 z(s,t)}{\partial t^2}+m\zeta\frac{\partial z(s,t)}{\partial t}+\epsilon\frac{\partial^4 z(s,t)}{\partial s^4}-\kappa\frac{\partial^2 z(s,t)}{\partial s^2}-\frac{W}{2}\left[3\left(\frac{\partial z}{\partial s}\right)^2-1\right]-F_0-zF_1=A(s,t). \quad (6)$$

The random thermal force for stiff chains satisfies the usual conditions;

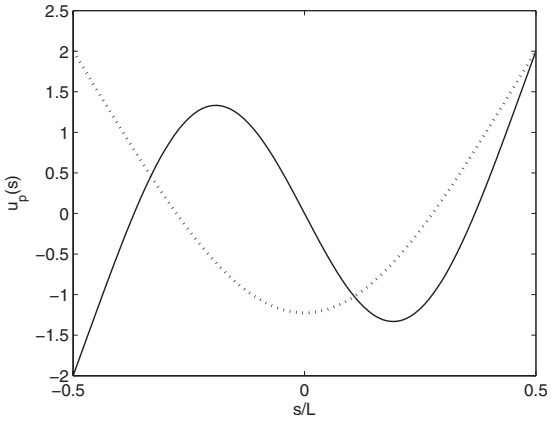

FIG. 1. Eigenfunctions of the bend and stretch elastic chain for $p=1$ (dashes) and 2 (line).

$$\langle A(s,t)\rangle = 0 \tag{7}$$

$$\langle A(s,t)A(s',t')\rangle = 4kTam\zeta\delta(t-t')\delta(s-s'). \tag{8}$$

Perpendicular to the pore axis in the x and y directions, the motion is that of a free chain $F_x=F_y=0$. Outside the pore, $W=0$ and $\vec{F}=e\vec{E}_0/\epsilon_s$.

B. Solution for the polymer modes

To investigate the dynamics including changes in conformation of the chain, an expansion in the bend eigenfunctions is used [38]:

$$z(s,t) = \sum_{p=0} u_p(s)q_p(t), \tag{9}$$

where $q_p(t)=\int ds\, z(s,t)u_p(s)/L$. The eigenfunctions $u_p(s)$ are solutions of

$$\epsilon\frac{\partial^4 u_p(s)}{\partial s^4} - \kappa\frac{\partial^2 u_p(s)}{\partial s^4} = (\epsilon\alpha_p^4 - \kappa\alpha_p^2)u_p(s) \tag{10}$$

and satisfy the boundary conditions for free ends of the polymer chain. The set of eigenfunctions is orthonormal: $\int ds\, u_p(s)u_{p'}(s)/L=\delta(p,p')$.

1. Case $p>0$

The eigenvalues are α_p and the eigenfunctions for $p>0$ are

$$u_p = c_0\exp(\alpha_p s) + c_1\exp(i\alpha_p s) + c_2\exp(-\alpha_p s) + c_1^*\exp(-i\alpha_p s). \tag{11}$$

The coefficients are found from minimization of the energy and normalization of the eigenfunctions. The eigenfunctions, shown in Fig. 1, are eigenfunctions of parity [21] and parity is conserved during translocation. In the dynamic equation (6) the driving force is invariant under the parity operation $s\to -s$. The eigenfunctions of parity $z(s)=\pm z(-s)$ are thus eigenfunctions of the dynamic equation [39]. The eigenvalues are determined by the boundary conditions.

For odd values of $p=1,3\ldots$, the functions are symmetrical:

$$u_p(s) = \cos(\alpha_p s)/(\cos\alpha_p L/2) + \cosh\alpha_p s/(\cosh\alpha_p L/2)$$

with

$$(\tan\alpha_p L/2)/(\tanh\alpha_p L/2) = -(\epsilon\alpha_p^2 - \kappa)/(\epsilon\alpha_p^2 + \kappa).$$

For even $p=2,4\ldots$, the functions are antisymmetrical:

$$u_p(s) = \sin(\alpha_p s)/(\sin\alpha_p L/2) + \sinh\alpha_p s/(\sinh\alpha_p L/2)$$

with

$$(\tan\alpha_p L/2)/(\tanh\alpha_p L/2) = (\epsilon\alpha_p^2 + \kappa)/(\epsilon\alpha_p^2 - \kappa).$$

The eigenvalues are well approximated by $\alpha_p=(2p+1)\pi/2L$. For odd parity, an additional eigenvalue is found at $\alpha_p=\pi/L$. This solution disappears for $\kappa=0$.

The equation of motion for the time-dependent functions $q_p(t)$ is found from Eq. (6). An expansion in the wall anchoring field is used to first order in W:

$$\frac{\partial^2 q_p(t)}{\partial t^2} + \zeta\frac{\partial q_p(t)}{\partial t} + [(\epsilon/m)\alpha_p^4 - (\kappa/m)\alpha_p^2 - F_1/m]q_p(t) = B_0(p,t) + B_1(p,t). \tag{12}$$

The frequency of the polymer mode $p>0$ is

$$\omega_{1,2}(p) = -\zeta/2 \pm \{\sqrt{\zeta^2 - 4[(\epsilon/m)\alpha_p^4 - (\kappa/m)\alpha_p^2 - F_1/m]}\}/2. \tag{13}$$

The solution for $q_p(t)$ for $p>0$ is

$$q_p(t) = \frac{1}{\omega_1(p)-\omega_2(p)}\left(\int dt'[B_0(p,t') + B_1(p,t')]\{\exp[\omega_1(p)\times(t-t')] - \exp[\omega_2(p)(t-t')]\} - q_p(0)\times\{\omega_2(p)\exp[\omega_1(p)t] - \omega_1(p)\exp[\omega_2(p)t]\} + \frac{\partial q_p(0)}{\partial t}\{\exp[\omega_1(p)t] - \exp[\omega_2(p)t]\}\right).$$

The fluctuating force is $B_0(p,t)=\int ds\, A(s,t)u_p(s)/mL$ and satisfies

$$\langle B_0(p,t)B_0(p',t')\rangle = 4\frac{kT\zeta}{mN}\delta(t-t')\delta(p,p').$$

An additional force arises from the fluctuations of q_p in the anchoring field: $(3W/2m)\int ds\, u_p(s)(\partial z/\partial s)^2/L$ with $\langle B_1(p,t)\rangle=(3W/2m)Q_pS_p(t)$. The related order parameter for odd p is $Q_p=\int ds\, u_p(s)(\partial u_p/\partial s)^2/L$. For even p, $Q_p=0$.

The time correlation function $S(p,p',t)=\langle q_p(t)q_{p'}(t')\rangle$ can be calculated using Eq. (12). The system becomes stationary after a time $\xi t\geqslant 1$ so that the correlation function for $\zeta t\gg 1$ is:

$$S(p,p',t\to\infty) = S(p) = \frac{4kTa}{L}(\epsilon\alpha_p^4 - \kappa\alpha_p^2 - F_1)^{-1}\delta(p,p').$$

2. Case $p=0$

A particular solution of the equation is given for $p=0$. From Eq. (6), the solution is $u_0(s)q_0(t)$ with $\epsilon\partial^4 u_0/\partial s^4$

$-\kappa\partial^2 u_0/\partial s^4=0$. Due to the boundary conditions $u_0(s)=1$ and $q_0(t)$ is the solution of

$$\frac{\partial^2 q_0(t)}{\partial t^2}+\zeta\frac{\partial q_0(t)}{\partial t}+W/2m-F_0/m-F_1 q(t)/m=B_0(t)+B_1(t). \tag{14}$$

The fluctuating force is again composed of two terms. The random white noise for the $p=0$ mode is $B_0(t)=\int ds\, A(s,t)/mL$. The fluctuating wall friction force for the $p=0$ mode is $B_1(t)=(3W/2m)\int ds(\partial z/\partial s)^2/L$. The orientation correlation in the z direction is given by $\sigma_p=\int ds[\partial u_p(s)/\partial s]^2/L$ and the average fluctuating force due to the anchoring field is $\langle B_1(t)\rangle=(3W/2m)\Sigma_{p=1}\sigma_p S_p(t)$. In the following $\langle B_1(t)\rangle=(3W/2m)\sigma$ with $\sigma=\Sigma_p\sigma_p S_p(t)$.

The frequencies are found from the equation of motion (14). For $F_1=0$, $\Omega_1=0$, $\Omega_2=-\zeta$. For $F_1\neq 0$,

$$\Omega_{1,2}=-\zeta/2\pm(\sqrt{\zeta^2+4F_1/m})/2. \tag{15}$$

For $F_1=0$ the solution for $q_0(t)$ is

$$q_0(t)=\frac{1}{\zeta}\left(\int dt'[F_0/m-W/2m+B_0(t')+B_1(t')]\{1-\exp[\zeta(t'-t)]\}+q_0(0)+\frac{\partial q_0(0)}{\partial t}[1-\exp(-\zeta t)]\right).$$

For $F_1<0$ the solution for $q_0(t)$ is

$$q_0(t)=\frac{1}{\Omega_1-\Omega_2}\left(\int dt'[B_0(t')+B_1(t')]\{\exp[\Omega_1(t-t')]-\exp[\Omega_2(t-t')]\}-q_0(0)[\Omega_2\exp(\Omega_1 t)-\Omega_1\exp(\Omega_2 t)]+\frac{\partial q_0(0)}{\partial t}[\exp(\Omega_1 t)-\exp(\Omega_2 t)]\right)-F_0/F_1+W/2F_1.$$

The dynamics of the macromolecule can now be discussed.

C. The polymer dynamics

The random motion of the elastic chain is superimposed on the orientation by the pore walls and drift caused by the electrostatic forces. The average motion of the center of mass is found from $Z_g(t)=\langle\int ds\, z(s,t)/L\rangle=\langle q_0(t)\rangle$. Using the initial conditions $Z_g(t=0)=Z_g(0)$, $\partial Z_g(t=0)/\partial t=v_0$, the center of mass at time t is located at

$$Z_g(t)=Z_g(0)+v_0[1-\exp(-\zeta t)]/\zeta+[F_0+W(3\sigma-1)/2]\times[\zeta t+\exp(-\zeta t)-1]/m\zeta^2 \tag{16}$$

for $F_1=0$, and for $F_1\neq 0$,

$$Z_g(t)=Z_g(0)\frac{\Omega_1\exp\Omega_2 t-\Omega_2\exp\Omega_1 t}{\Omega_1-\Omega_2}+\frac{v_0(\exp\Omega_1 t-\exp\Omega_2 t)}{\Omega_1-\Omega_2}+\left(\frac{\Omega_1\exp\Omega_2 t-\Omega_2\exp\Omega_1 t}{\Omega_1-\Omega_2}-1\right)\times[F_0/F_1+W(3\sigma-1)/2F_1].$$

As the polymer diffuses through the pore the initial velocity decays and the average monomer velocity $\langle\int ds\, v(s)\rangle/L=\partial Z_g(t)/\partial t$ contains a contribution from the pore wall interaction.

A measure of the extension along z is the z component of the center to end distance vector: $R_z(t)=\langle z(L/2,t)-z(0,t)\rangle$ so that $R_z(t)=\Sigma_{p=1}[u_p(L/2)-u_p(0)]\langle q_p(t)\rangle$. The initial orientation is chosen to be isotropic, $R_z(0)=0$ and $dR_z/dt=0$. Using Eqs. (10) and (12), we calculate

$$R_z(t)=\frac{3W}{2m}\sum[u_p(L/2)-u_p(0)]\frac{Q_p S(p)}{\omega_1(p)\omega_2(p)}\times\left(\frac{\omega_2(p)\exp[\omega_1(p)t]-\omega_1(p)\exp[\omega_2(p)t]}{\omega_1(p)-\omega_2(p)}+1\right).$$

For short times $t\zeta<1$ the extension is defined by the initial conditions:

$$R_z(t)=R_z(0)+t\frac{\partial R_z(0)}{\partial t},$$

and at long times $t\zeta\gg 1$, R_z reaches a constant value $R_z(\infty)$,

$$R_z(\infty)=3W\sum_{p=1}[u_p(L/2)-u_p(0)]\frac{S(p)Q_p}{\epsilon(\alpha_p)^4-\kappa(\alpha_p)^2-F_1}.$$

The initial monomer positions and initial polymer conformation are not fixed. The initial conditions are needed only for average chain properties. Here, the center of gravity $Z_g(0)$ is positioned at $-L/2$ from the pore entrance and the average velocity of the pore chain is $dZ_g(0)/dt=v_0$. Translocation is said to occur at $t=\tau$ when $Z_g(\tau)=H+L$ and most of the polymer chain has exited the pore. The total pore field is set to zero outside the pore. Time-dependent effects are not considered in the narrow transition region close to the pore exit and entrance, where some of the chain is under the influence of the pore electric field but does not yet sense orientation by wall atoms. The assumption is used that on entering the pore the stationary average orientation of each monomer is established rapidly within ξ^{-1}.

III. DISCUSSION

A. Effect of chain elasticity

The dynamics of flexible stretch elastic chains are well known: the normal modes are given by a Fourier series with appropriate boundary conditions $u_p(s)=\cos(p\pi s/L)$. The equilibrium average $\langle\langle\cdots\rangle\rangle$ of the mode coordinates determines the stretch elastic coefficient of the p mode from eq-

uipartition [13]; the end to end distance is $\langle\langle R^2\rangle\rangle = La$ and $\kappa = kT/3$.

Bend elasticity adds the exponential functions to describe the polymer modes and a typical conformation, given in Eq. (11), is shown in Fig. 1. Here the zero-order "rigid rod" mode proportional to s is the solution of zero bend energy and maximum stretch energy and is not retained [17,40,41]. For semirigid chains, the stretch elastic coefficient is set to zero and the chain avoids bend deformations by increasing the effective size of the polymer chain. In the wormlike chain model, only those chain conformations that satisfy the condition of constant length or $|d\vec{r}/ds| = 1$ are considered in the calculation of the probability distribution [15]. The bend elastic coefficient is determined from the equilibrium distribution of $\langle\langle q_p^2\rangle\rangle$ for $t \to \infty$ and the equilibrium end to end distance is found. The bend elastic coefficient is then simply related to the correlation length b of the chain orientation: $\epsilon = kTba$. In the rigid chain limit, $L/b < 1$; the persistence length b is large and the end to end distance of the bend chain is calculated as $\langle\langle R^2\rangle\rangle/L^2 \approx 1$. In DNA the persistence length is given as $b/a = 80$, and using $b = 56$ nm and $a = 0.7$ nm from the molecular dynamics simulation to which results will be compared, then $b/L = 4$, $L/a = 20$[11].

The intermediate case of finite stretch and bend has been investigated [5–7,17–19,21] and by use of the appropriate eigenfunctions chain dynamics were studied in the presence of external fields. The bend elastic constant changes the time evolution of the polymer modes with a strong dependence of the frequency on L^4 and not L^2 as for stretch polymers. Finite stretch combined with bend modifies the frequencies and decay times of the polymer modes. The equilibrium end to end distance is found as $\langle\langle R^2\rangle\rangle = (3kTa/L)\Sigma_p(\epsilon\alpha_p^4 - \kappa\alpha_p^2)^{-1}$.

For weak bend, $\epsilon/\kappa L^2 \ll 1$, the end to end distance of stretch elastic chains is recovered. In the case of rigid chains with strong bend, $\epsilon/(\kappa L^2) \gg 1$, the contributions from the bend and stretch modes compensate [19,21] and the end to end distance is determined mainly by the antisymmetric mode $\alpha_p L = \pi$. Setting $\langle\langle R^2\rangle\rangle = L^2$ the bend elastic coefficient $\epsilon = 6kT(32aL/\pi^4)$ is then found to lie close to the value of DNA in the simulation. From $\epsilon/kT = ab$, the value $b/L = 2$ will be used here with $L/a = 20$. Equilibrium properties of bend elastic chains in the stationary limit of the normal mode analysis will not be equivalent to the same quantities calculated in the wormlike chain model since an average over conformations with a different set of restrictions is performed. The two approaches will be equal only if the sampling in both cases is sufficiently thorough to capture typical behavior. The parameter σ is a measure of the deviation from the geometric wormlike chain model.

B. Effect of friction

The effective friction coefficient determines the decay times for polymer dynamics on entering and leaving the pore. The value can be estimated from the diffusion constant $D = kT/m\zeta$ of the single chain of degree of polymerization L/a in the relevant solvent. Neglect of the hydrodynamic interaction is justified for sufficiently wide pores. From a reasonable value of diffusion constant $D = 10^{-6}$ cm^2 s^{-1} and monomer mass $m = 10^{-21}$ g, the monomer friction coefficient is found to be of the order of 10^{13} s^{-1}. A good fit of simulation to experimental results was found for $\xi = 10^{16}$ s^{-1} [42].

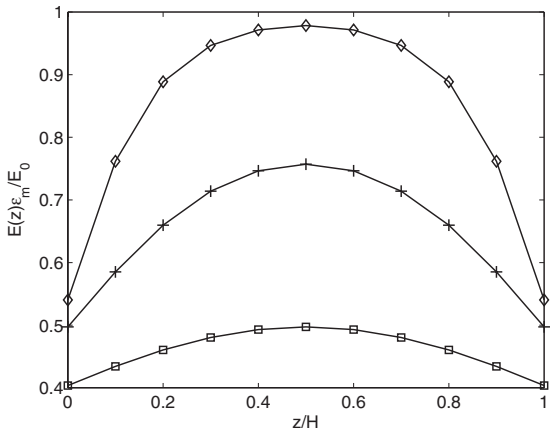

FIG. 2. Induced pore electric field $E(z)$ relative to the applied electric field in a solvent of dielectric constant ϵ_s as a function of distance z on the pore axis for different pore geometries $R/H = 0.2$ (diamonds), 0.5 (crosses), and 1 (squares) for $\epsilon_m/\epsilon_s = 0.05$. The pore dimensions are R, radius; H, height. The membrane dielectric constant is ϵ_m.

C. Effect of electric field

The electric field inside the pore is given by Eq. (3) and plotted in Fig. 2. The similarity with the field obtained by molecular dynamics (MD) simulation [11] for a synthetic nanopore is visible and the scaling law in $E(z)/E_0 = f(z/H)$ is satisfied. A small variation of the gradient of the electric field in z justifies the expansion used in the calculation and is shown in Fig. 3.

In the simulation $R/H = 0.2$ and the variation of the electric field gradient is large, as shown in Fig. 3. In order to accelerate the translocation from milliseconds to nanoseconds, the applied voltage of the simulation is 1.4 V; typically

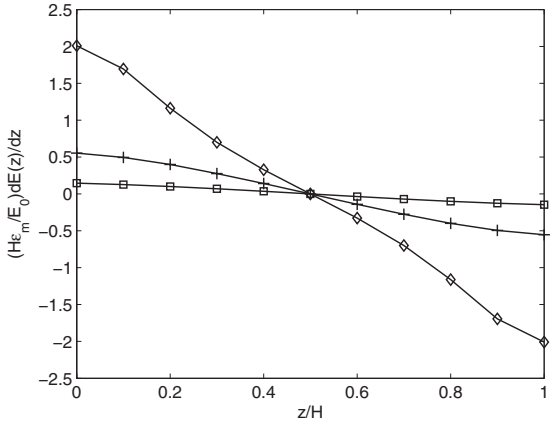

FIG. 3. Gradient $dE(z)/dz$ of the induced pore electric field $E(z)$ relative to the applied electric field in the solvent of dielectric constant ϵ_s as a function of distance z on the pore axis for different pore geometries $R/H = 0.2$ (diamonds), 0.5 (crosses), and 1 (squares). The pore dimensions are R, radius; H, height.

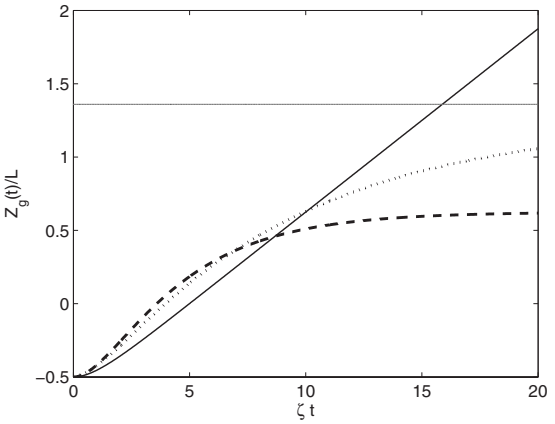

FIG. 4. Motion of the center of mass Z_g/L of the polymer of length L as a function of time ζt and for different values of stiffness of the optical trap: $F_1/m\zeta^2=0$ (line), −0.1 (dots), and −0.2 (dashes). The straight upper line corresponds to the translocation time. $F_0/mL\zeta^2=0.125$, $W/mL\zeta^2=10^{-3}$.

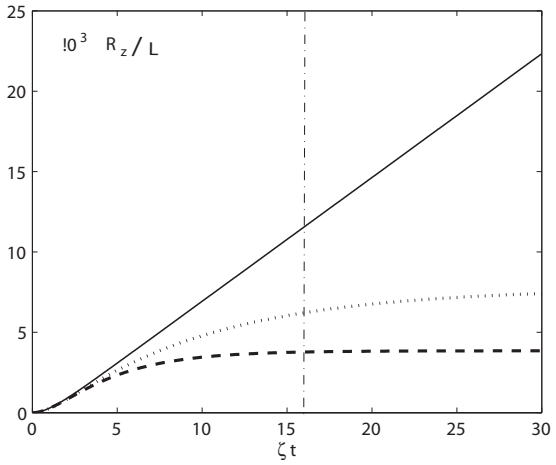

FIG. 5. Projection R_z/L of the center to end distance of the polymer of length L $(L/a=20)$ as a function of time ζt and for different values of stiffness of the optical trap: $F_1/m\zeta^2=0$ (line), −0.1 (dots), −0.2 (dashes) in a wall potential $W/(mL\zeta^2)=10^{-3}$. The dash dot line corresponds to the translocation time.

in experiments a voltage of the order of millivolts is applied [11]. To compare results, values of $F_0/eE_0=0.12$, $F_1H/eE_0=-7$, and $E_0=10^6$ V/cm are obtained from the simulation and $F_0/eE_0=0.1$, $F_1H/eE_0=-0.33$ from Eq. (3) for $H=5$ nm, $R=1$ nm. Outside the pore, chain translation is due to acceleration by the uniform applied field and the chain arrives at the pore entrance with a velocity $v_0=eE_0/\epsilon_s m\zeta$. The motion of the center of mass of the chain inside the pore is plotted in Fig. 4. The chain motion is initially linear in time, and after a time ζ^{-1} the chain motion is driven by the internal pore field with a velocity $v_\infty=F_0/m\zeta+W(3\sigma-1)/2m\zeta$.

The large electric force of the simulation dominates the translation of the chain through the pore and in particular the field gradient over the uniform field. The translocation time τ is measured by the time for the center of mass to exit the pore with $Z_g(\tau)=H+L$ and $\tau=m\zeta(H+L)/F_0$. The translocation time is inversely proportional to the applied field and proportional to the polymer length as found in experiment. Outside the pore, the velocity of the polymer center of mass returns to the value v_0 within ζ^{-1}.

For experimental fields of the order of 1 V/cm or less, the dynamics are dominated by the force due to the pore wall, the motion is linear in time with $v_\infty=W(3\sigma-1)/2m\zeta$, and translocation times of the order of microseconds are obtained.

Experiments have been made in the presence of an optical trap placed at the end of the pore [1]. A field is created proportional to the distance of the chain to the pore end as given by the term in F_1. The optical trap affects the chain velocity and the time needed to block the polymer within the pore is smaller the larger the strength of the trap. The chain motion shown in Fig. 4 is initially linear in time but stops at a finite stationary value after a time $t_c=m\zeta/(-F_1)$, inversely proportional to the field constant F_1, and which in the present model of independent monomer motion does not depend on the ratio of pore size to polymer length. If the chain exits the pore before this time is reached, then the translocation time is calculated from the initial velocity as $\tau=(\epsilon m\zeta)(H+L)/eE_0$. Then, as before, the translocation time is inversely proportional to the applied field and proportional to the polymer length.

D. Effect of the pore walls

The interaction with the pore walls accelerates the translation of the polymer chain and contributes to the motion of the center of mass. For strong bend and weak stretch, the order parameter is calculated from Eq. (10):

$$\sigma=\sum_{p\ \text{even}}(\alpha_p^2+3\alpha_p/L)S(p)+\sum_{p\ \text{odd}}(\alpha_p^2+4\alpha_p/L)S(p)+[(\pi/L)^2+3\pi/(L^2)]S(\pi/L).$$

The contribution from the odd-parity mode with $\alpha_p=\pi/L$ again dominates. For the parameters of the DNA simulation, σ lies close to 0.4 and for $W/mL\zeta^2=10^{-3}$ the velocity term from the pore wall friction is an order of magnitude smaller than that of the induced electric field in the pore. The wall friction affects the polymer conformation and the extension of the chain increases in the z direction. The order parameter is calculated as $Q_p=2\alpha_p(1+\cosh\alpha_pL)/(5L\cosh\alpha_pL/2)$. The evolution with time of the projection of the center to end vector along the pore axis is plotted in Fig. 5 (parameters as in Fig. 4). The extension initially increases slowly with time; the rapidly damped vibrations due to the polymer modes are not shown. The frequencies of the vibrating polymer modes for large p are $\Omega_p^2=(\epsilon/m)(\alpha_p)^4$ so that $\Omega_p=(2p+1)^2\times10^6$ s^{-1}. After a time of the order of $\omega_1(p=1)^{-1}$, a fixed finite value of the projection is reached, which depends on the effective wall interaction. After exiting the pore the extension decays to the value of free chains $R_z=0$ within a time ζ^{-1}. The maximum average extension of the polymer on exiting the pore at τ is about 0.01 of the chain length for a friction force $W/m\zeta^2L=10^{-3}$. These values correspond to an average of the center to end vector projected onto the pore axis; local order may be much greater. For large pores it was

shown in a molecular dynamics simulation [10] that ordering of the polymer is large mainly when the chain is located a few nanometers from the pore walls. The extension consists here of orientation of the monomers as well as a change of monomer length. For experimental fields of the order of 1 V/cm or less, linear time dependence of the chain extension is again rapidly established and $\partial R_z/\partial t = 3WL/2bm\zeta$. Large extension of the polymer chain is possible due to translocation times of the order of microseconds.

In the presence of the optical trap, the stationary chain extension is reached in a time inversely proportional to the field constant $t_c \approx \zeta m/(-F_1)$. The extension R_z is blocked at a value given by the ratio $W/(-F_1)$ of the wall force to the field strength. For $F_1/m\zeta^2 = -0.1$ the maximum extension is 0.5% and the time needed to block the chain and reach maximum extension is close to the translocation time τ as seen in Fig. 4.

IV. CONCLUSIONS

In this paper we have examined the motion of a semirigid polymer in a nanopore. The improvements of the present model go beyond the flexible model by simply increasing the effective monomer length (or decreasing the stretch elasticity) to a value consistent with the persistence length. In contrast to flexible polymers described by a stretch elasticity, bend elastic chains can be oriented in an external field, here the anchoring field created by the pore atoms. For anchoring of the polymer parallel to the pore axis, the walls of the pore must not be smooth. Surface roughness is consistent with the complex potential profiles of synthetic and natural pores where internal sites, trapped charges, and complex structure occur. For example, silicon dioxide surfaces can have a negative charge density possibly neutralized by counterion condensation. The mean field approximation assumed for the wall interaction requires that temporary adsorption of monomers onto the pore walls translates into an effective average force suitable if a sufficient number of weak, rapidly fluctuating bonds is created during passage through the pore. In narrow pores with strong interaction with the polymer, the variation of the adsorption potential perpendicular to the pore walls along x and y is not negligible. Motion of the monomers along the pore axis is affected and cannot be decoupled as in the present model.

The transition time for the polymer to pass through the nanopore is determined mainly by the electric field within the pore and the effective pore wall interaction. The drift through the pore is superimposed on random damped motion of the monomers and a continuous change of conformation. The electric field gradient inside the pore couples to the dipoles of the chain and decreases the time required for translocation inside the pore. In a strong electric field gradient, exploitation of the effect of the different base dipole moments on the polymer dynamics appears feasible. Application of a force proportional to the distance of the exit to the end of the pore such as an optical trap slows down the motion, and reduces the chain response to the wall potential and the extension along the pore axis. This technique in combination with more complex pore geometry may prove useful in future nanopore studies.

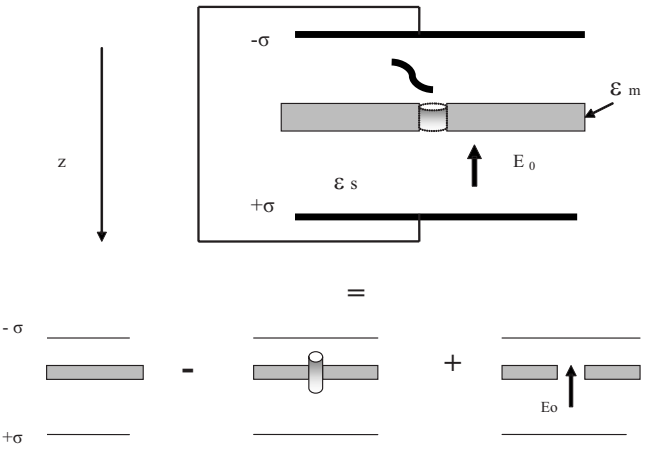

FIG. 6. The components of the electric field within the pore.

A vast amount of experimental, theoretical and simulation work exists for DNA translocation. The two approaches of phenomenological modeling (as used here) and molecular dynamics are complementary. On the one hand, the phenomenological description of polymer dynamics makes it possible to study dependence on important parameters of the system such as pore length, geometry, and applied field, even for long times. But for more detailed knowledge such as the effect of atomistic structure a description based on molecular dynamics on short time scales cannot be avoided.

DNA is a well-known semirigid polymer and Langevin dynamics based on bend elasticity should provide a good qualitative picture and help to determine optimal conditions for a given experiment.

APPENDIX

The set up is given in Fig. 6. The field is approximated by the field induced by surface charges on the upper and lower plates superimposed on the dielectric cavity formed by the pore.

First the membrane of dielectric constant ϵ_m is replaced by charged surfaces at separation H with induced charge $\pm\sigma$ on the upper and lower surfaces. The cylinder of radius R, charged on upper and lower disk surfaces, is removed to form the pore and then replaced by the applied electric field E_0 in the dielectric medium of dielectric constant ϵ_s.

[1] M. Zwolak and M. DiVentra, Rev. Mod. Phys. **80**, 141 (2008).
[2] J. Lagerqvist, M. Zwolak, and M. DiVentra, Biophys. J. **93**, 2384 (2007).
[3] K. Luo, I. Huopaniemi, T. AlaNissala, and S. Ying, J. Chem. Phys. **124**, 114704 (2006).
[4] C. Forrey and M. Muthukumar, J. Chem. Phys. **127**, 015102 (2007).
[5] J. Wang and H. Gao, J. Chem. Phys. **123**, 084906 (2005).
[6] J. Wang and H. Gao, J. Mater. Sci. **42**, 8838 (2007).
[7] L. X. Zhang, A. Xia, and D. Zhao, Eur. Polym. J. **37**, 1277 (2001).
[8] Y. L. Chen, M. D. Graham, J. J. DePablo, G. C. Randall, M. Gupta, and P. S. Doyle, Phys. Rev. E **70**, 060901(R) (2004).
[9] K. Luo, T. Ala-Nissala, S. C. Ying, and A. Bhattacharya, Phys. Rev. Lett. **99**, 148102 (2007).
[10] F. Zhang, J. Chem. Phys. **111**, 9082 (1999).
[11] J. Heng, A. Aksimentiev, C. Ho, P. Marks, Y. Grinkova, S. Sligar, K. Schulten, and G. Timp, Biophys. J. **90**, 1098 (2006).
[12] M. Gracheva, A. Xiong, A. Aksimentiev, K. Schulten, G. Timp, and J. Leburton, Nanotechnology **17**, 622 (2006) ;http://www.ks.uiuc.edu/Research/nanopore
[13] M. Doi and S. Edwards, *The Theory of Polymer Dynamics* (Oxford Science, Oxford, 1986).
[14] M. Bawendi and K. Freed, J. Chem. Phys. **83**, 2491 (1985).
[15] A. ten Bosch, Makromol. Chem., Theory Simul. **2**, 851 (1993).
[16] P. Benetatos and E. Frey, Phys. Rev. E **70**, 051806 (2004).
[17] R. Harris and J. Hearst, J. Chem. Phys. **44**, 2595 (1966).
[18] N. Saito, K. Takahashi, and Y. Yunoki, J. Phys. Soc. Jpn. **22**, 219 (1967).
[19] K. Soda, J. Phys. Soc. Jpn. **35**, 866 (1973).
[20] A. C. Maggs, Phys. Rev. Lett. **85**, 5472 (2000).
[21] S. Aragon and R. Pecora, Macromolecules **18**, 1868 (1985).
[22] B. Jerome, Rep. Prog. Phys. **54**, 391 (1991).
[23] A. ten Bosch, Phys. Rev. E **63**, 061808 (2001).
[24] L. I. Klushin, A. M. Skvortsov, and F. A. M. Leermakers, Phys. Rev. E **66**, 036114 (2002).
[25] P. A. Wiggins, T. van der Heijden, F. Moreno-Herrero, A. Spakowitz, R. Phillips, J. Widom, C. Dekker, and P. Nelson, Nat. Nanotechnol. **1**, 137 (2006).
[26] P. Maissa and A. ten Bosch, J. Polym. Sci., Part C: Polym. Lett. **24**, 481 (1986).
[27] G. Ronca and A. ten Bosch, *Liquid Crystallinity in Polymers* (Wiley, New York, 1991).
[28] R. M. Jendrejack, E. T. Dimalanta, D. C. Schwartz, M. D. Graham, and J. J. DePablo, Phys. Rev. Lett. **91**, 038102 (2003).
[29] M. Robbins and J. Krim, MRS Bull. **23**(6), 23 (1998).
[30] J. Dzubiella and J. Hansen, J. Chem. Phys. **122**, 234706 (2005).
[31] E. Durand, *Electrostatique I* (Masson, Paris, 1964).
[32] K. Levin, Europhys. Lett. **76**, 163 (2006).
[33] Y. Rabin and M. Tanaka, Phys. Rev. Lett. **94**, 148103 (2005).
[34] S. Ghosal, Phys. Rev. E **74**, 041901 (2006).
[35] N. Madhusudana and S. Chandrasekhar, in *Proceedings of the International Conference on Liquid Crystals*, edited by S. Chandrasekhar [Pramana **1**, 57 (1973)].
[36] T. Barrett, Phys. Lett. **94A**, 59 (1983).
[37] M. Fixman, J. Chem. Phys. **76**, 6346 (1982).
[38] J. Rayleigh, *The Theory of Sound* (Dover Publications, New York, 1945).
[39] S. Morse and H. Feshbach, *Methods of Theoretical Physics* (McGraw-Hill, New York, 1953).
[40] L. D. Landau and E. M. Lifshitz, *Theory of Elasticity*, Theoretical Physics Vol. 7 (Butterworth Heinemann, Oxford, 1986).
[41] S. F. Mingaleev, Y. Gaididei, P. Christiansen, and Y. S. Kivshar, Europhys. Lett. **59**, 403 (2002).
[42] S. Matysiak, A. Montesi, M. Pasquali, A. B. Kolomeisky, and C. Clement, Phys. Rev. Lett. **96**, 118103 (2006).